



Glacier shrinkage in the Alps continues unabated as revealed by a new glacier inventory from Sentinel-2

Frank Paul¹, Philipp Rastner¹, Roberto Sergio Azzoni², Guglielmina Diolaiuti², Davide Fugazza², Raymond Le Bris¹, Johanna Nemec³, Antoine Rabaté⁴, Mélanie Ramusovic⁴, Gabriele Schwaizer³, Claudio Smiraglia²

⁸ 1 Department of Geography, University of Zurich, Zurich, Switzerland

⁹ 2 Department of Environmental Science and Policy, University of Milan, Milan, Italy

10 3 ENVEO IT GmbH, Innsbruck, Austria

4 Univ. Grenoble Alpes, CNRS, IRD, Grenoble-INP, Institut des Géosciences de l'Environnement
12 (IGE, UMR5001), Grenoble, France

Correspondence: Frank Paul (frank.paul@geo.uzh.ch)

15 Abstract

The on-going glacier shrinkage in the Alps requires frequent updates of glacier outlines to provide an accurate database for monitoring or modeling purposes (e.g. determination of run-off, mass balance, or future glacier extent) and other applications. With the launch of the first Sentinel-2 (S2) satellite in 2015, it became possible to create a consistent, Alpine-wide glacier inventory with an unprecedented spatial resolution of 10 m. Fortunately, already the first S2 images acquired in August 2015 provided excellent mapping conditions for most of the glacierised regions in the Alps. We have used this opportunity to compile a new Alpine-wide glacier inventory in a collaborative team effort. In all countries, glacier outlines from the latest national inventories have been used as a guide to compile a consistent update. However, cloud cover over many glaciers in Italy required including also S2 scenes from 2016. Whereas the automated mapping of clean glacier ice was straightforward using the band ratio method, the numerous debris-covered glaciers required intense manual editing. The uncertainty in the outlines was determined with multiple digitising of 14 glaciers by all participants. Topographic information for all glaciers was derived from the ALOS AW3D30 DEM. Overall, we derived a total glacier area of $1806 \pm 60 \text{ km}^2$ when considering 4394 glaciers $>0.01 \text{ km}^2$. This is 14% (-1.2%/a) less than the 2100 km^2 derived from Landsat scenes acquired in 2003 and indicating an unabated continuation of glacier shrinkage in the Alps since the mid-1980s. Due to the higher spatial resolution of S2 many small glaciers were additionally mapped in the new inventory or increased in size compared to 2003. An artificial reduction to the former extents would thus result in an even higher overall area loss. Still, the uncertainty assessment revealed locally considerable differences in interpretation of debris-covered glaciers, resulting in limitations for change assessment when using glacier extents digitised by different analysts. The inventory is available at: doi.pangaea.de/10.1594/PANGAEA.909133 (Paul et al., 2019).



38

39 **1. Introduction**

40 Precise information on glacier extents is required for numerous glaciological and hydrological cal-
41 culations, ranging from the determination of glacier volume, surface mass balance and future glaci-
42 er evolution to run-off, hydro-power production, and sea-level rise (e.g., Marzeion et al., 2017).
43 For these and several other applications glacier outlines spatially constrain all calculations thus
44 providing an important baseline dataset. In response to the on-going atmospheric warming, glaci-
45 ers retreat, shrink and lose mass in most regions of the world (e.g., Gardner et al. 2013, Wouters et
46 al. 2019, Zemp et al. 2019). Accordingly, a frequent update of glacier inventories is required to
47 reduce uncertainties in subsequent calculations. With relative area loss rates of about 1% per year
48 in many regions globally (Vaughan et al. 2013), glaciers lose about 10% of their area within a dec-
49 ade and a decadal update frequency seems sensible. In regions with stronger glacier shrinkage such
50 as the tropical Andes (e.g. Rabaté et al. 2013, 2018) or the European Alps (e.g. Gardent et al.
51 2014) an even higher update frequency is likely required. However, apart from the high workload
52 required to digitise or manually correct glacier outlines (e.g. Racoviteanu et al. 2009), it is often
53 not possible to obtain satellite images in a desired period of the year with appropriate mapping
54 conditions, i.e. without seasonal snow and clouds hiding glaciers. Hence, glacier inventories are
55 often compiled from images acquired over several years resulting in a temporarily inhomogeneous
56 dataset. Fortunately, a 3-year period of acquisition is still acceptable in error terms, as area chang-
57 es of about $\pm 2\%$ are within the typical area uncertainty of about 3 to 5% (e.g. Paul et al. 2013).

58

59 The last glacier inventory covering the entire Alps with a common and homogeneous date has
60 been compiled from Landsat Thematic Mapper (TM) images acquired within six weeks in the
61 summer of 2003 (Paul et al. 2011). Although this dataset has its caveats (e.g. missing small glaci-
62 ers in Italy and some debris-covered ice), it is methodologically and temporally consistent and
63 representing glacier outlines of the Alps in the Randolph Glacier Inventory (RGI). A few years
64 later, high quality glacier inventories were compiled from very high-resolution datasets (aerial
65 photography, airborne laser scanning) on a national level in all four countries of the Alps with sub-
66 stantial glacier coverage (Austria, France, Italy, Switzerland). These more recent inventories refer
67 to the periods 2008-2011 for Switzerland (Fischer et al. 2014), 2004-2011 for Austria (Fischer et
68 al. 2015), 2006-2009 for France (Gardent et al. 2014), and 2005-2011 for Italy (Smiraglia et al.
69 2015). As an 8-year period is rather long, consistent and comparable change assessment is chal-
70 lenging. However, for the first version of the World Glacier Inventory (WGI) the temporal spread
71 was even larger, ranging from 1959 to about 1983 (Zemp et al. 2008). Another problem for change
72 assessment is the inhomogenous interpretation of glacier extents, in part to be compliant with the
73 analysis in earlier inventories. Hence, calculations over the entire Alps that require a consistent
74 time stamp are difficult to perform and rates of glacier change are difficult to compare across re-
75 gions (e.g. Gardent et al. 2014).



76

77 Considering the on-going strong glacier shrinkage in the Alps over the past decades and the above
78 shortcomings of existing datasets, there is a high demand to compile a (1) new, (2) precise and (3)
79 consistent glacier inventory for the entire Alps, with data acquired under (4) good mapping condi-
80 tions in (5) a single year. Although it might be difficult to satisfy all five criteria at the same time,
81 at least some of them seem achievable by means of recently available satellite data. With the 10 m
82 resolution data from Sentinel-2 (S2) and its 290 km swath width it is possible (a) to improve the
83 quality of the derived glacier outlines (compared to Landsat TM) substantially (Paul et al. 2016)
84 and (b) to cover a region such as the Alps with a few scenes acquired within a few weeks or even
85 days, satisfying criteria (2) and (5). Good mapping conditions, however, only occur by chance af-
86 ter a comparably warm summer when all seasonal snow off glaciers has melted and largely cloud
87 free conditions persist over an extended time span in August or September.

88

89 In this study we present a new glacier inventory for the European Alps that has been compiled
90 from S2 data that were mostly acquired within two weeks of August 2015 (during the commission-
91 ing phase). However, due to glaciers (mostly in Italy) being partly cloud-covered, also scenes
92 from 2016 (and very few from 2017) were used. Hence, criterion (5) could not be fully satisfied. In
93 order to satisfy point (3), we decided to perform the mapping of clean ice with an identical method
94 (band ratio), and distribute the raw outlines to the national experts for editing of wrongly classified
95 regions (e.g. adding missing ice in shadow and under local clouds or debris cover, removing lakes
96 and other water surfaces). As a guide for the interpretation the analysts used the latest high-
97 resolution inventory in each country. All corrected datasets were merged into one dataset and
98 topographic information for each glacier was derived from the ALOS AW3D30 DEM. For uncer-
99 tainty assessment all participants corrected the extents of 14 glaciers independently four times.

100

101 **2. Study region**

102 The Alps are a largely west-east (south-north in the West) oriented mountain range in the centre of
103 Europe (roughly from 2° to 18° E and 43° to 49° N) with peaks reaching 4808 m a.s.l. in the West
104 at Mt. Blanc/Monte Bianco and elevations above 3000 m a.s.l. in most regions. In Fig. 1 we show
105 the region covered by glaciers along with footprints of the tiles used for data processing. The Alps
106 act thus as a topographic barrier for air masses coming from the North and South as well as from
107 the West in the western part. This results in enhanced orographic precipitation and a high regional
108 variability of precipitation amounts in specific years as well as in the long-term mean (e.g. Frei et
109 al. 2003). On the other hand, temperatures are horizontally rather uniform (e.g. Böhm et al. 2001)
110 but vary strongly with height according to the atmospheric lapse rate (e.g. Frei 2014). Snow accu-
111 mulation is mostly due to winter precipitation, but some snowfall can also occur in summer at
112 higher elevations, reducing ablation for a few days.

113



114 There is no significant long-term trend in precipitation over the last 100+ years (Casty et al. 2005),
115 but summer temperatures in the Alps have increased sharply (by about 1 °C) in the mid-1980s (e.g.
116 Beniston 1997, Reid et al. 2016). In consequence, winter snow cover barely survives the summer
117 even at high elevations and / or when strong positive deviations in temperature occurred. Glacier
118 mass balances in the Alps were thus pre-dominantly negative over the past three decades (e.g.
119 Zemp et al. 2015) and the related mass loss resulted in widespread glacier shrinkage and disinte-
120 gration over the past decades (e.g. Gardent et al. 2014, Paul et al. 2004). With a total area of about
121 2000 km² in 2003 and a mean annual mass loss of about 1 m w.e. per year, the European Alps cur-
122 rently lose about 2 Gt of ice per year.

123

124 Most glaciers in the Alps are of cirque, mountain and valley type and the two largest ones (Aletsch
125 and Gorner glaciers) have an area of about 80 km² and 60 km², respectively. Some glaciers reach
126 down to 1300 m a.s.l., and the overall mean elevation is around 3000 m a.s.l., a unique value com-
127 pared to other regions of the RGI (e.g. Pfeffer et al. 2014). Due to the surrounding often ice-free
128 rock walls of considerable height, many glaciers in the Alps are heavily debris-covered. Whereas
129 this allowed the tongues of several large valley glaciers to survive at comparably low elevations
130 (Mölg et al. 2019), many glaciers - large and small - become invisible under increasing amounts of
131 debris. Combined with the on-going down-wasting and disintegration, precisely mapping their ex-
132 tents is increasingly challenging.

133

Figure 1

134

135

136 **3. Datasets**

137 **3.1 Satellite data**

138 In total, 23 S2 tiles were processed to cover the study region with cloud free images (Figure 1 and
139 Table 1). Of these, 11 were acquired in 2015, 9 in 2016 and 3 in 2017. Convective clouds in Italy
140 (mostly along the Alpine main divide) required stretching the main acquisition period over two
141 years. All glaciers in France were mapped from four tiles acquired on 29.8.2015. This date covers
142 also most glaciers mapped in Switzerland (five tiles) apart from the south-east tile 32TNS that was
143 acquired three days earlier (26.8.2015). Three tiles from that date (32TNT / TNS / TPT) are used
144 to map glaciers in western-Austria and three tiles (32TQT / 32TQS / 33TUN) from 27.8.2016 for
145 the eastern part of Austria. Twelve tiles had to be used to map glaciers in Italy of which two are
146 from 2015, seven are from 2016, and three from 2017 (Fig. 1). However, the latter three only cov-
147 er very few and small glaciers so that collectively the northern (Switzerland / Austria) and western
148 (France) parts of the inventory are from 2015 whereas the southern (Italy) and eastern (Austria)
149 parts are from 2016. All tiles were downloaded from remotepixel.ca (only the required bands, no
150 longer possible), earthexplorer.usgs.gov or the Copernicus Open Access Hub.

151



Table 1

152
153
154 From all tiles, bands 2, 3, 4, 8, and 11 (blue, green, red, Near Infra-Red / NIR, Short Wave Infra-
155 Red / SWIR) of the sensor Multi Spectral Imager (MSI) were downloaded and colour composites
156 were created from the 10 m visible and NIR (VNIR) bands. The 20 m SWIR band 11 was bilinear-
157 ly resampled to 10 m resolution to obtain glacier outlines at this resolution. The 10 m resolution
158 VNIR bands allowed for a much better identification of glacier extents (e.g. correcting debris-
159 covered parts) than possible with Landsat (Paul et al. 2016), resulting in a higher quality of the
160 outlines. Apart from the resampling, all image bands are used as they are except for Austria, where
161 further pre-processing has been applied (see Section 4.2.1). The August 2015 scenes from the S2
162 commissioning phase had reflectance values stretched from 1 to 1000 (12 bit) instead of the later
163 16 bit (allowing values up to 65536), but this linear rescaling had no impact on the threshold value
164 for the band ratio (see Section 4.1).

165

166 **3.2 Digital elevation models (DEMs)**

167 We originally intended using the new TanDEM-X (TDX) DEM to derive topographic information
168 for all glaciers, as it covers the entire Alps and was acquired closest (around 2013) to the satellite
169 images used to create the inventory. However, closer inspection revealed that it had data voids and
170 suffered from severe artefacts (Fig. 2). Although these are mostly located in the steep terrain out-
171 side of glaciers, many smaller glaciers are severely impacted, resulting in wrong topographic in-
172 formation. As an alternative we investigated the ALOS AW3D30 DEM that was compiled from
173 ALOS tri-stereo scenes (Takaku et al. 2014) and acquired about five years before the TDX DEM
174 (around 2008). The AW3D30 DEM has a less good temporal match but no data voids and compa-
175 rably few artefacts (Fig. 2). The individual tiles were merged into one 30 m dataset in UTM 32N
176 projection with WGS84 datum. For the pre-processing of satellite bands in Austria, a national
177 DEM with 10 m resolution derived from laser scanning was used (Open Data Österreich: da-
178 ta.gv.at).

179

Figure 2

180

181

182 **3.3 Previous glacier inventories**

183 As mentioned above, outlines from previous national glacier inventories were used to guide the
184 delineation. They have been mostly compiled from aerial photography with very high spatial reso-
185 lution (better than 1 m) and should thus provide the highest possible quality. This allowed consid-
186 ering very small and otherwise unnoticed glaciers and helped to identify glacier zones that are de-
187 bris covered. The substantial glacier retreat that took place between the two inventories was well
188 visible in most cases and did not hamper the interpretation. However, a larger number of very
189 small glaciers were not mapped in 2003 and have now been added or digitised with larger extents.
190 A large issue with respect to additional work load is the compilation of ice divides. They can be



191 derived semi-automatically from watershed analysis of a DEM using a range of methods (e.g.
192 Kienholz et al. 2013), but in general numerous manual corrections have still to be applied. To pro-
193 vide some consistency with previous national inventories, we decided using the drainage divides
194 from these inventories to separate glacier complexes into entities. However, due to the locally poor
195 geolocation of the S2 scenes (Kääb et al. 2016, Stumpf et al. 2018), the location of the ice divides
196 was partly manually adjusted.

197

198 4. Methods

199 4.1 Mapping of clean ice in all regions

200 Automated mapping of clean to slightly dirty glacier ice is straight forward using a red or NIR to
201 SWIR band ratio and a (manually selected) threshold (e.g. Paul et al. 2002). Also other methods
202 such as the normalised difference snow index (NDSI) work well (e.g. Racoviteanu et al. 2009) as
203 both utilise the strong difference in reflectance from the VNIR to the SWIR for snow and ice (e.g.
204 Dozier 1989). As the latter are bright in the VNIR bands (high reflectance) but very dark (low re-
205 flectance) in the SWIR, dividing a VNIR band by a SWIR band gives high values over glacier ice
206 and snow and very low ones over all other terrain as this is often much brighter in the SWIR than
207 the VNIR. The manual selection of a threshold for each scene (or S2 tile) has the advantage to in-
208 clude a regional adjustment of the threshold to local atmospheric conditions. We followed the rec-
209 ommendation to select the threshold in a way that good mapping results in regions with shadow
210 are achieved. By lowering the threshold, more and more bare rock in shadow is included, creating
211 a very noisy result. It has been shown in a previous study (Paul et al. 2016) that glacier mapping
212 with S2 (using a red / SWIR ratio) requires an additional threshold in the blue band to remove
213 misclassified rock in shadow. Hence, for this inventory glaciers have been first automatically iden-
214 tified following the equation:

215

$$216 \quad (\text{red} / \text{SWIR}) > th1 \text{ and } \text{blue} > th2$$

217

218 with the empirically derived thresholds $th1$ and $th2$. As mentioned above, the SWIR band was bi-
219 linearly resampled from 20 to 10 m spatial resolution before computing the ratio. No filter for im-
220 age smoothing was applied to retain fine spatial details, such as rock outcrops. Figure 3 shows for
221 a test site in the Mt. Blanc region (Leschaux Glacier) the impact of the threshold selection. Figure
222 3a depicts the (contrast stretched) red / SWIR ratio image, Fig. 3b the impact of $th1$ on the mapped
223 area, Fig. 3c the impact of $th2$, and Fig. 3d the resulting outlines after raster-vector conversion. As
224 can be seen in Fig. 3b, there is very little impact on the mapped glacier area when increasing $th1$ in
225 steps of 0.2. For this region we used 3.0 as $th1$ resulting in the blue and yellow areas as the
226 mapped glacier. Wrongly mapped rock in shadow is then reduced back with $th2$ (Fig. 3c). In this
227 case a value of 860 was selected for $th2$ i.e. only the blue area is considered. This correctly re-



228 moved rock in shadow from the glacier mask for the region to the right of the white arrow but, on
229 the other hand, correctly mapped ice in shadow is removed at the same time in the region above
230 the green arrow (Figs. 3c and d). Hence, threshold selection is always a compromise as it is in gen-
231 eral not possible to map everything correctly with one set of thresholds. The resulting glacier maps
232 for all regions were converted to a shape file using raster-vector conversion and by setting the non-
233 glacier class to ‘*no data*’ before. In the resulting shape file internal rocks are thus data voids.
234
235 All pre-processed scenes were provided in their original geometry for correction by the national
236 experts. As shown in Fig. 3c, it was sometimes not possible to include dark bare ice and at the
237 same time exclude bare rock in shadow. Such wrongly classified regions were corrected by the
238 analysts together with data gaps for debris cover and clouds (omission errors), wrongly mapped
239 water bodies (e.g. turbid lakes and rivers) and shadow regions (commission errors). By setting the
240 minimum glaciers size to 0.01 km², most of the often very small snow patches were removed.

241
242 *Figure 3*
243

244 **4.2 Corrections in the different countries**

245 **4.2.1 Austria**

246 The satellite scenes for Austria were further pre-processed (see Paul et al. 2016) to remove water
247 surfaces and improve classification of glacier ice in cast shadow, before manual corrections were
248 applied. The latter work was mainly performed by one person (J. Nemec). Two previous Austrian
249 glacier inventories (Lambrecht and Kuhn 2007, Fischer et al. 2015) were used to support the inter-
250 pretation of small glaciers, debris covered glacier parts, and the boundary across common accumu-
251 lation areas. Further, an internal independent quality control of the generated glacier outlines was
252 made by a second person (G. Schwaizer), using orthophotos (30 cm pixel spacing) acquired in late
253 August 2015 for most Austrian glaciers for overall accuracy checks and to assure the correct delin-
254 ection of debris covered glacier areas. In Fig. 4a we illustrate the strong glacier shrinkage from
255 1998 (yellow lines) to 2016 (red) as well as the manual corrections applied, extending the bright
256 filled areas of the raw classification to the red extents.
257

258 **4.2.2 France**

259 The raw glacier outlines from S2 were corrected by one person (A. Rabatel). The glacier outlines
260 from the previous inventory by Gardent et al. (2014) were used for the interpretation, in particular
261 in shadow regions and for glaciers under debris cover. It is noteworthy that the previous inventory
262 was made on the basis of aerial photographs (2006-2009) with field campaigns for the debris-
263 covered glacier tongues to clarify the outline delineation. As a consequence, this previous invento-
264 ry constitutes a highly valuable reference. In addition, because even on debris-covered glaciers the
265 changes between 2006-09 and 2015 are important (Fig. 4b), Pléiades images from 2015-2016 ac-
266 quired within the KALIDEOS-Alpes / CNES program were used as a guideline, mostly for the



267 heavily debris-covered glacier tongues.

268

269 **4.2.3 Italy**

270 The raw glacier outlines from S2 were corrected by two analysts (D. Fugazza, R.S. Azzoni). The
271 outlines were separated into regions based on the administrative division of Italy, following the
272 previous Italian glacier inventory (Smiraglia et al. 2015). From west to east, the regions are Aosta
273 Valley, Piemonte, Lombardy, Trento Province, Bolzano Province, Veneto, Friuli, Venezia Giulia.

274

275 As mentioned in the Introduction, clouds covered the southern Alpine sector on the S2 scenes from
276 August 2015. Hence, most of the inventory was compiled based on images from August and Sep-
277 tember 2016 and 3 scenes from 2017 (one in August and two in October) were also used to map
278 glaciers that were under clouds or with adverse mapping conditions, i.e. excessive snow cover or
279 shadows in the other scenes. Images acquired in August had little residual seasonal snow and a
280 high solar elevation at the time of acquisition, which minimised shadow areas creating very good
281 mapping conditions. In September 2016 and October 2017, more snow was present on high moun-
282 tain cirques and glacier tongues, but comparatively few snow patches were found outside glaciers.
283 However, the lower solar elevation compared to August caused a few north-facing glaciers and
284 glacier accumulation areas to be under shadows.

285

286 Seasonal snow and rocks in shadow that were wrongly identified as clean ice were manually delet-
287 ed by the analysts, as well as lakes and large rivers. In shadow regions, and for glaciers with large
288 debris cover, the outlines from the previous Italian inventory by Smiraglia et al. (2015) were par-
289 ticularly valuable as a guide. Where glaciers were entirely under shadows, the outlines from the
290 previous inventory were copied without changes, while in case of partial shadow coverage they
291 were edited in their visible portions.

292

293 Glaciers in three sectors of the Alps, i.e. the Orobic Alps, Dolomites and Julian Alps posed signifi-
294 cant challenges for mapping. The three regions host very small niche glaciers and glacierets: in the
295 Orobic and Julian Alps, their survival is granted by abundant snow-falls, northerly aspect and ac-
296 cumulation from avalanches, with debris cover also playing an important role. In the Dolomites,
297 debris cover is often complete (Smiraglia and Diolaiuti 2015), while the steep rock walls provide
298 shadow and further complicate mapping.

299

300 For glaciers in the Orobic Alps, an aerial orthophoto acquired by Regione Lombardia (geopor-
301 tale.regione.lombardia.it) in 2015 was used to aid the interpretation in view of its finer spatial reso-
302 lution, although the image also shows evidence of seasonal snow. Here, manual delineation of the
303 glacier outlines was required as the band ratio approach could only detect small snow patches (see
304 Fig. 4c). In the other two regions, outlines from the previous inventory, derived from aerial ortho-



305 photos acquired in 2011, were copied and only corrected where evidence of glacier retreat was
306 found. While the uncertainty in the outlines of these latter glaciers is likely large, the combined
307 glacier area from the three regions is just above 1% of the total area of Italian glaciers.

308

309 **4.2.4 Switzerland**

310 The raw glacier outlines from S2 were corrected by three persons (R. LeBris, F. Paul, P. Rastner)
311 each of them being responsible for a different main region (south of Rhone, north of Rhone/Rhine,
312 south of Rhine). The glacier outlines from the previous inventory by Fischer et al. (2014) were
313 highly valuable for the interpretation, in particular in shadow regions and for glaciers under debris
314 cover. In the hot summer of 2015 most seasonal snow had disappeared by the end of August so
315 that mapping conditions with a comparably high solar elevation (limited regions in shadow) were
316 very good. Some glaciers that could not be identified in the (contrast-stretched) S2 images were
317 either copied from the previous inventory (if located in shadow) or assumed to have disappeared
318 (if sun-lit). Wrongly mapped (turbid) lakes and rivers (Rhone, Aare) were manually removed.

319

320 In a few cases (mostly debris-covered glaciers) we had to deviate from the interpretation of the
321 previous inventories. As shown in Fig. 4d, very high-resolution satellite imagery (as sometimes
322 available in Google Earth) or aerial photography do not always help for a ‘correct’ interpretation
323 of glacier extents, as the rules applied for identification of ice under debris cover might differ. In
324 this case it seems that the debris-covered region was not corrected in the 2003 and 2008 invento-
325 ries, but is now largely included. This glacier has thus strongly grown since 2003 due to a new in-
326 terpretation and the better visibility of debris cover with S2.

327

328 *Figure 4*

329

330 **4.3. Drainage divides and topographic information**

331 Drainage divides between glaciers were copied from previous national inventories but were locally
332 adjusted along national boundaries. In part this was required because different DEMs had been
333 used in each country to determine the location of the divide. Additionally, some glaciers are divid-
334 ed by national boundaries rather than flow divides. This can result in an arbitrary part of the glaci-
335 er (e.g. its accumulation zone) being located in one country and the other part (e.g. its ablation
336 zone) in another country. As this makes no sense from a glaciological (and hydrological) point of
337 view, such glaciers (e.g. Hochjochferner in the Ötztal Alps) have been corrected in a way that they
338 belong to the country where the terminus is located. There are thus a few inconsistencies in this
339 inventory compared to the national ones.

340

341 After digital intersection of glacier outlines with drainage divides, topographic information for
342 each glacier entity is calculated from both DEMs (ALOS and TDX) following Paul et al. (2009).
343 The calculation is fully automated and applies the concept of zone statistics introduced by Paul et



344 al. (2002). Each region with a common ID (this includes regenerated glaciers consisting of two
345 polygons) is interpreted as a zone over which statistical information (e.g. minimum / maximum /
346 mean elevation) is derived from an underlying value grid (e.g. a DEM or a DEM-derived slope and
347 aspect grid). Apart from glacier area (in km²) all glaciers have information about mean, median,
348 maximum and minimum elevations, mean slope and aspect (both in degrees) and aspect sector
349 (eight cardinal directions) using letters and numbers (N=1, NE=2, etc.). Further information ap-
350 pended to each glacier in the attribute table of the shape file is the satellite tile used, the acquisition
351 date, the analyst and the funding source. This information is applied automatically by digital inter-
352 section ('*spatial join*') to all glaciers from a manually corrected scene footprint shape file (see Fig.
353 1). The various attributes have then been used for displaying key characteristics of the datasets in
354 bar graphs, scatter plots and maps (see Section 5.1).

355

356 **4.4 Change assessment**

357 Glacier area changes have only been calculated with respect to the inventory from 2003, as the
358 dates for the previous national inventories were too diverse for a meaningful assessment (see In-
359 troduction). To obtain consistent changes, only glaciers that are also mapped in the 2003 inventory
360 are used for a direct comparison (automatically selected via a '*point in polygon*' check). After real-
361 ising that a glacier-specific comparison is not possible due to differences in interpretation, we de-
362 cided to only compare the total glacier area of the previous and new inventory.

363

364 **4.5 Uncertainty assessment**

365 As several analysts have digitised the new inventory, we decided performing multiple digitising of
366 a pre-selected set of glaciers to determine internal variability in interpretation per participant and
367 across participants as a measure of the uncertainty of the generated dataset. For this purpose, all
368 participants used the same raw outlines from S2 tile 32TLR to manually correct 14 glaciers (sizes
369 from 0.1 to 10 km²) to the south of Lac des Dix around Mt. Blanc de Cheilon (3870 m a.s.l.) for
370 debris cover. All glaciers were digitised 4 times by 5 participants giving a nominal total of 280
371 outlines for comparison. Results were analysed using an overlay of outlines to identify the general
372 deviations in interpretation and through a glacier-by-glacier comparison of glacier sizes. For the
373 latter all datasets were intersected with the same drainage divides and glacier-specific areas were
374 calculated. For each glacier and the entire region, mean area values and standard deviations are
375 calculated per glacier, per participant and for the total sample. The participants were asked to only
376 use the S2 image and the 2003 outlines as a guide for interpretation in the first two digitisation
377 rounds and consider interpretation of very high-resolution imagery as provided by Google Earth
378 for the second two rounds. At a minimum, one day should have passed between each digitisation
379 round and it was not allowed to show any of the former outlines. On average, each digitisation
380 round took about 2 hours.

381



382 Additionally, we applied the buffer method to obtain a statistical uncertainty value for the entire
383 sample. This method gives a minimum and maximum area and was used to determine a relative
384 area difference. This value multiplied by 0.68 gives the standard deviation (assuming normally
385 distributed deviations from the correct outline) that is used as a further measure of area uncertainty
386 (Paul et al. 2017). The selected buffer is based on an earlier multiple digitising experiment for a
387 couple of glaciers (Paul et al. 2013) showing that the variability in the positioning is within one
388 pixel (or about ± 10 m in the current case) to both sides of the ‘true’ vector line. Strictly, a larger
389 buffer should be used for the debris-covered glacier parts, as their uncertainty is higher. However,
390 we have not implemented this here, as the related calculations are computationally expensive (cf.
391 Mölg et al. 2018). Instead, we also applied a ± 2 pixels buffer to all glaciers. Depending on the de-
392 gree of debris coverage, a realistic uncertainty estimate is likely between these two values.
393

394 **5. Results**

395 **5.1 The new glacier inventory**

396 In total, we identified 4394 glaciers larger than 0.01 km^2 covering a total area of 1805.77 km^2 , of
397 which 361.5 km^2 (20%) is found in Austria and 227.1 (12.6%), 325.3 (18%), and 892.0 km^2
398 (49.4%) in France, Italy, and Switzerland, respectively. The size class distribution by area and
399 count is depicted in Fig. 5a and also listed in Table 2. In total, 63% (92%) of all glaciers are small-
400 er than 0.1 km^2 (1.0 km^2) covering 5.5% (28%) of the glacierised area, whereas 1.6% are larger
401 than 5 km^2 and cover 40%. Thereby, glaciers in the size class 1 to 5 km^2 alone cover one third
402 (32%) of the area but only 6% of the total number. This biased size class distribution is typical for
403 alpine glaciers where a few large glaciers are surrounded by numerous much smaller ones. The
404 distribution of glacier number and area by aspect sector displayed in Fig. 5b shows the dominance,
405 both in number and coverage area, of northerly exposed glaciers compared to all other sectors.
406 About 60% of all glaciers (covering 60% of the area) are exposed to the NW, N, or NE whereas
407 only 21% of all glaciers are found in the sectors SE, S, and SW. This distribution of glacier aspects
408 is typical for regions where radiation plays a larger role in glacier existence compared to factors
409 such as precipitation (Evans and Cox, 2005). The larger area coverage for glaciers facing SE is
410 mostly due to the large Aletsch and Fiescher glaciers.

411
412 *Figure 5, Table 2*
413

414 A plot of glacier surface area vs. minimum and maximum elevations (Fig. 6a) reveals that glaciers
415 smaller than 1 km^2 can be found at all elevations, indicating that their mean elevation does only
416 slightly depend on climatic factors. Glaciers larger than 1 km^2 on the other hand have clearly dis-
417 tinguished maximum and minimum elevations, *i.e.* they arrange around a climatically driven mean
418 elevation which is around 3000 m a.s.l. Plotting glacier area vs. elevation range (Fig. 6b) shows
419 that the largest glaciers are not those with the highest elevation range (the maximum of 3140 m is



420 for Glacier des Bossons in the Mont-Blanc massif with a size of 10 km²) and that for the majority
421 of glaciers the elevation range increases with glacier size. This is typical for regions dominated by
422 mountain and valley glaciers as these follow the given topography. The ca. 7 km² large Plaine
423 Morte Glacier is a plateau glacier with an elevation range of only 350 m and represents an excep-
424 tion from the rule.

425
426 *Figure 6*
427

428 The median elevation of a glacier is largely driven by temperature, precipitation and radiation. As
429 temperature is rather similar at the same elevation over large regions and topography (aspect /
430 shading) has a strong local impact on radiation receipt, the large-scale variability of median (or
431 mean) elevation of a glacier has a high correlation with precipitation amounts (e.g. Ohmura et al.
432 1992, Oerlemans 2005, Rastner et al. 2012, Sakai et al. 2015). The spatial distribution of glacier
433 median elevations in the Alps (Fig. 7a) thus also reflects the general pattern of annual precipitation
434 amounts (e.g. Frei et al. 2003). When focusing on glaciers larger than 0.5 km² (that are less im-
435 pacted by local topographic conditions), clearly lower median elevations (around 2400 m a.s.l.) are
436 found for glaciers along the northern margin of the Alps and major mountain passes than in the
437 inner Alpine valleys (around 3700 m a.s.l.) that are well shielded from precipitation. On top of this
438 variability comes the variability due to a different aspect (Fig. 7b): On average, glaciers that are
439 exposed to the south have median elevations that are about 400 m higher (at 3200 m a.s.l.) than
440 north-facing glaciers (at 2800 m a.s.l.). However, the scatter is high and for each aspect the eleva-
441 tion variability is about 1500 m.

442
443 *Figure 7*
444

445 The graph in Fig. 8 shows the hypsometry of glacier area in the four countries and for the total ar-
446 ea in relative terms. On average, the highest area share is found around the mean elevation of 3000
447 m a.s.l. By referring for each country to the total area as 100%, differences among them can be
448 seen. Most notable is the smaller elevation range and larger peak of glaciers in Austria, the broader
449 vertical distribution in Switzerland (with the lowest peak value), and the slightly higher peak of the
450 distribution in Italy (at 3100 m a.s.l.). The hypsometry of glaciers in France is closest to the curve
451 for the entire Alps.

452
453 *Figure 8*
454

455 **5.2 Area changes**

456 For a selection of 2873 glaciers present in both inventories, total glacier area shrunk from 2060
457 km² in 2003 to 1783 km² in 2015/16 or by -13.2% (-1.1%/a). Considering the assumed missing
458 area in the 2003 inventory of about 40 km² (glaciers with area gain are 29.4 km² larger in 2015/16
459 than in 2003), a more realistic area loss is -15% or -1.3%/a. This is about the same pace as report-



460 ed earlier by Paul et al. (2004) for the Swiss Alps from 1985 to 1998/99 (-1.4%/a). An example of
461 the strong glacier shrinkage in Austria is depicted in Fig. 9. Closer inspection of this image also
462 reveals the small shift (to the SE) of the S2 scenes compared to the earlier Landsat TM scenes.

463
464 *Figure 9*
465

466 The comparison of glacier outlines in Fig. 10 illustrate for the region around Sonnblickkees in
467 Austria why we do not provide a scatterplot of relative area changes vs. glacier size or country
468 specific area change values (cf. also Fig. 4d for Gaviolas Glacier in Switzerland). Due to the dif-
469 ferent interpretations in the new inventory, 125 mostly very small glaciers are 100% to 630% larg-
470 er than in 2003 and a large number (557) is 0% to 100% larger. For example, the 4 km² Suldenfer-
471 ner has increased in size by 550% as a small tributary (that holds the ID for the glacier) was dis-
472 connected in 2003 but is now connected to the entire glacier. Although such cases can be manually
473 adjusted, it would not solve the general problem of the different interpretation. For example, the
474 glacier in Fig. 4d has increased its size from 2003 to 2015 by 56% due to the new interpretation.
475 On the other hand, Careser glacier, which fragmented in six ice bodies from 2003 to 2015, lost
476 55% of its area when summing up all parts as opposed to 63% when considering the largest glacier
477 only. In consequence, the possible area reduction due to melting is partly compensated by the more
478 generous interpretation of glacier extents and thus with a limited meaning on the basis of individu-
479 al glaciers. Assuming that some glaciers in 2015/16 are larger due to included seasonal snow, the
480 real area loss would be even higher than the previously estimated -15%.

481
482 *Figure 10*
483

484 **5.3 Uncertainties**

485 **5.3.1 Glacier outlines**

486 The multiple digitising experiment revealed several interesting albeit well-known results. Overall,
487 the area uncertainty (one standard deviation, STD) is 3.3% across all participants for the total of
488 the digitised area (Table 3). As two glaciers (11 and 13) were not mapped by one participant, the
489 missing values are replaced with the mean value from the other participants. Across all glaciers but
490 for individual participants the uncertainty (comparing the values from the four digitisation rounds)
491 is considerably lower (1% to 2.7%), indicating that the digitising is more consistent when per-
492 formed by the same person. The area values of participant 1 (P1) are systematically higher than for
493 the other participants, about 6% for the total area. A detailed analysis of the digitised outlines (Fig.
494 11) revealed that the differences are mostly due to the more generous inclusion of debris-covered
495 glacier ice for two of the larger glaciers (Nr. 1 and 5). When excluding P1, the STD across the oth-
496 er participants is three times smaller (1.1%). The uncertainty also slightly depends on glacier size,
497 showing values between 1% and 6% for glaciers larger than 1 km² and between 2% and 20% for
498 glacier <1 km². The smallest glacier in the sample is smaller than 0.1 km² and shows variations in
499 STD between 8% and 44%, in the latter case also due to a reinterpretation of its extent when using



500 very high-resolution imagery. For such small glaciers related changes can thus result in considera-
501 bly different extents.

502
503 *Table 3, Figure 11*
504

505 Moreover, for P1 and most of the other participants the digitised glacier extents increased by sev-
506 eral per cent after consultation of very high-resolution satellite images as available in Google Earth
507 and the aerial imagery from the swisstopo map server. The generally very flat and debris-covered
508 regions were barely visible on the S2 images and have been digitised very differently in each of
509 the four rounds. Hence, the possibility for a re-interpretation of the outlines within the same exper-
510 iment resulted in higher standard deviations. If such regions have to be included in a glacier inven-
511 tory or not can be discussed, as the transition to ice-cored medial or lateral moraines is often grad-
512 ual and including these features in a glacier inventory or not is a (personal) methodological deci-
513 sion. However, it points to an underestimation of glacier area also with 10 m resolution sensors
514 and confirms earlier recommendations to double-check all digitised glacier extents with such very
515 high-resolution sensors, at least for ‘difficult’ glaciers (e.g. Fischer et al. 2014).

516
517 The uncertainty (one STD) obtained with the buffer method is $\pm 5\%$ (10%) when using a 10 m (20
518 m) buffer. This is in line with the mean values of the uncertainties derived from the multiple digit-
519 ising experiment and numerous previous studies.

520
521 **5.3.2 Topographic information**

522 The comparison of minimum, maximum and mean glacier elevation as well as mean slope and
523 aspect derived from the TDX and AW3D30 DEM, revealed in particular towards smaller glaciers
524 larger differences. Smaller glaciers are more likely to be impacted by artefacts as these easily share
525 a large percentage of their total area. Differences in mean slope and aspect are generally small but
526 increase towards larger slope values for the former. This is in agreement with the general observa-
527 tions that DEM quality is reduced at steep slopes. Minimum elevation is slightly higher in the
528 TDX DEM, which can be explained by glacier retreat between the acquisition dates. However, a
529 clearly lower mean elevation due an overall surface lowering of the glaciers could not be observed,
530 indicating that the differences are in the uncertainty range. Apart from artefacts, the uncorrected
531 radar penetration of the TDX DEM might play a role here as well.

532

533 **6. Discussion**

534 The derived size class distribution (Fig. 5) and topographic information are typical for glaciers in
535 mid-latitude mountain ranges with numerous smaller glaciers surrounding a few larger ones. Only
536 354 out of 4394 glaciers (8%) are larger than 1 km² and nearly one half (46%) is smaller than 0.05
537 km² covering 2.7% of the area. It might be well possible that many of the latter are no longer glac-



538 iers but just perennial snow and firn patches. However, for consistency with earlier inventories
539 they have been included. Mean elevation values do not really depend on glacier size for such gla-
540 ciers, indicating that they can survive at different elevations and precipitation amounts have a lim-
541 ited impact. If they are well protected from solar radiation (e.g. by shadow or debris cover) such
542 glaciers might persist for some time despite increasing air temperatures. Glacier mean elevation
543 (about 3000 m a.s.l.) does not depend on glacier size but is modified by glacier location with re-
544 spect to precipitation sources and mean aspect, in particular for larger glaciers (Fig. 7).

545

546 Widespread glacier thinning and steep terrain resulted lately in interrupted profiles for several
547 larger valley glaciers whose lower parts are no longer nourished by ice from above. In other
548 words, these parts are not regenerated glaciers but melt away as dead ice. Strictly speaking, such
549 lower dead ice bodies (that can persist due to debris cover for a very long time) should be excluded
550 from a glacier inventory (Raup and Khalsa 2007). However, for consistency with former invento-
551 ries and their contribution to run-off we included them here and merged their IDs to obtain more
552 reasonable topographic information for the combined extent. Calculating this instead for the indi-
553 vidual parts would result in related outliers and a more difficult analysis of trends. At best, such
554 separated parts are identified with a flag in the attribute table, for example as a further extension to
555 the ‘Form’ attribute (e.g. ‘4: Separated glacier part’) used in the RGI (RGI consortium 2017).
556 However, the differentiation from a regenerated glacier might sometimes be difficult.

557

558 Due to the differences in interpretation (Fig. 10) we have not compared the 2003 extents of indi-
559 vidual glaciers directly with those from the new inventory but only the total area of glaciers ob-
560 served in both inventories. Considering the underestimated glacier area in 2003 (e.g. due to miss-
561 ing debris cover) and possibly overestimated sizes in 2015 (e.g. due to included snow) the pace of
562 shrinkage (-1.3% /a) has not changed compared to the earlier mid-1980s to 2003 period. This indi-
563 cates that most glaciers have not yet reached a geometry that is compliant with current climate
564 conditions and will thus continue shrinking in the future. This becomes also clear from the snow
565 cover remaining near the end of the ablation period on the glaciers, covering barely 20% to 30% of
566 the area (e.g. Figs. 9 and 11). Assuming a required 60% coverage of their accumulation area, gla-
567 ciers in the Alps have to lose another 50% to 70% of their area to reach again balanced mass budg-
568 ets (Carturan et al. 2013). There are other regions in the world with similar high (or even higher)
569 area loss rates such as the tropical Andes (e.g. Rabaté et al. 2013), but to a large extent this is also
570 due to the smaller glaciers in this region. A realistic comparison across regions would only be pos-
571 sible when change rates of identical size classes are compared.

572

573 The multiple digitising experiment (Fig. 11) revealed a large variability in the interpretation of de-
574 bris-covered glaciers among the analysts but high consistency in the corrections where boundaries
575 are well visible. Related area uncertainties can be high for very small glaciers (>20%) but are gen-



576 really <5%. The here derived area reduction of about -15% since 2003 is thus significant, but for
577 small and/or debris-covered glaciers the area uncertainty can be similar to the change, making it
578 less reliable. However, this strongly depends on the specific glacier characteristics and cannot be
579 generalized to all small glaciers.

580

581 The gradual disappearance of ice under debris cover and the separation of low-lying glacier
582 tongues on steep slopes are major problems for any glacier inventory created these days. We de-
583 cided to re-connect disconnected glacier parts by their ID (to so-called *multi-part polygons*) for
584 consistency with earlier inventories. However, keeping them separated is another possibility, given
585 that possible dead ice is clearly marked in the attribute table.

586

587 **7. Conclusions**

588 We presented the results of a new glacier inventory for the entire Alps derived from Sentinel-2
589 images of 2015 and 2016. In total, 4394 glaciers >0.01 km² covering an area of 1806 ±60 km² are
590 mapped. This is a reduction of about 300 km² or -15% (-1.3%/a) compared to the previous Alpine-
591 wide inventory from 2003. The pace of glacier shrinkage in the Alps remained about the same
592 since the mid-1980's, indicating that glaciers will continue to shrink under current climatic condi-
593 tions. Due to the differences in interpretation, we have not performed a glacier-by-glacier compari-
594 son of area changes. The on-going glacier decline also results in increasingly difficult glacier iden-
595 tification (under debris cover) and topologic challenges for a database (when glaciers split). The
596 former is confirmed by the results of the uncertainty assessment, showing a large variability in the
597 interpretation of glacier extents when conditions are challenging. Despite the additional workload,
598 we think this is the best way to provide an uncertainty value for such a highly corrected and
599 merged dataset. In any case, the outlines from the new inventory should be more accurate than for
600 2003, as we here used the previous, high-quality national inventories as a guide for interpretation,
601 performed corrections by the respective experts, and worked with the higher resolution of Senti-
602 nel-2 data that helped in identifying important spatial details.

603

604 The clean-ice mapping with the band ratio method is straightforward, but requires well-thought
605 decisions on the two thresholds as they will always be a compromise. They should be tested in re-
606 gions with ice in cast shadow and selected in a way that the workload for manual corrections is
607 minimised. If a precise DEM is available, the required corrections of wrongly mapped ice in shad-
608 ow can be reduced as the further pre-processing for glaciers in Austria revealed. However, reduced
609 DEM quality and co-registration issues as well as local illumination differences can limit the bene-
610 fits of a topographic normalisation of the images. Due to the artefacts in the first version of the
611 TanDEM-X DEM, we used the ALOS AW3D30 DEM to derive topographic information for each
612 glacier despite the less good temporal agreement. To conclude, we had much better datasets avail-
613 able for this inventory compared to the 2003 dataset, but for several reasons (e.g. debris cover,



614 clouds, seasonal snow) the creation of glacier inventories from satellite data and a DEM remains a
615 challenging task with high workload and expert knowledge required.
616

617 **8. Data availability**

618 The dataset can be downloaded from: <https://doi.pangaea.de/10.1594/PANGAEA.909133> (Paul et
619 al., 2019).

620

621 **Author contributions**

622 FP designed the study, prepared the raw glacier outlines, performed various calculations and wrote
623 the manuscript. PR performed most of the GIS-based calculations and the editing that was required
624 to obtain a complete dataset and change assessment (e.g. drainage divides, satellite footprints,
625 country boundaries, DEM mosaicking and co-registration, dataset merging, topographic data). All
626 authors processed, corrected and checked the created glacier outlines in their country and contrib-
627 uted to the contents and editing of the manuscript. FP, DF, JN, AR, and PR performed the multiple
628 digitising of glacier outlines for uncertainty assessment.
629

630 **Competing interest**

631 The authors declare that they have no conflict of interests.
632

633 **Acknowledgements**

634 This study has been performed in the framework of the project Glaciers_cci (4000109873/14/I-
635 NB) and the Copernicus Climate Change Service (C3S) that is funded by the European Union and
636 implemented by ECMWF. R.S. Azzoni and D.Fugazza were funded by DARA - Department for
637 regional affairs and autonomies of the Italian presidency of the council of Ministers (funding code
638 COLL_MIN15GDIOL_M) and Levissima Sanpellegrino S.P.A., (funding code
639 LIB_VT17GDIOL). For the French Alps contribution, A. Rabatel and M. Ramusovic acknowledge
640 the *Service National d'Observation GLACIOCLIM* (Univ. Grenoble Alpes, CNRS, IRD, IPEV,
641 <https://glacioclim.osug.fr/>), the LabEx OSUG@2020 (*Investissements d'avenir* – ANR10
642 LABX56), the EquipEx GEOSUD (*Investissements d'avenir* – ANR-10-EQPX-20), the CNES /
643 Kalideos Alpes and CNES / SPOT-Image ISIS program #2011-513 for providing the Pléiades im-
644 ages and SPOTDEM from 2011. For the Austrian Alps, G. Schwaizer and J. Nemec acknowledge
645 funding from the Environmental Earth Observation (ENVEO) IT GmbH and the Austrian Re-
646 search Promotion Agency (FFG) within the ASAP9-SenSAP project (3574408).

647



648 References

- 649 Beniston, M., Diaz, H.F., and Bradley, R.S.: Climatic change at high elevation sites: A review,
650 *Climatic Change*, 36, 233-251, 1997.
- 651 Böhm, R., Auer, I., Brunetti, M., Maugeri, M., Nanni, T., and Schöner, W.: Regional temperature
652 variability in the European Alps 1760–1998 from homogenized instrumental time series, *International, Journal of Climatology*, 21, 1779-1801, 2001.
- 653
- 654 Carturan, L., Filippi, R., Seppi, R., Gabrielli, P., Notarnicola, C., Bertoldi, L., Paul, F., Rastner, P.,
655 Cazorzi, F., Dinale, R., and Dalla Fontana, G.: Area and volume loss of the glaciers in the Ort-
656 les-Cevedale group (Eastern Italian Alps): Controls and imbalance of the remaining glaciers,
657 *The Cryosphere*, 7, 1339-1359, 2013.
- 658 Casty, C., Wanner, H., Luterbacher, J., Esper, J., and Böhm, R.: Temperature and precipitation
659 variability in the European Alps since 1500, *International Journal of Climatology*, 25 (14),
660 1855-1880, 2005.
- 661 Dozier, J.: Spectral signature of alpine snow cover from Landsat 5 TM, *Remote Sensing of Envi-
662 ronment*, 28, 9-22, 1989.
- 663 Evans, I.S., and Cox, N.J.: Global variations of local asymmetry in glacier altitude: Separation of
664 north-south and east- west components, *Journal of Glaciology*, 51 (174), 469-482, 2005.
- 665 Fischer, M., Huss, M., Barboux, C., and Hoelzle, M.: The new Swiss Glacier Inventory SGI2010:
666 Relevance of using high-resolution source data in areas dominated by very small glaciers, *Arc-
667 tic, Antarctic and Alpine Research*, 46(4), 933-945, 2014.
- 668 Fischer, A., Seiser, B., Stocker-Waldhuber, M., Mitterer, C., and Abermann, J.: Tracing glacier
669 changes in Austria from the Little Ice Age to the present using a lidar-based high-resolution
670 glacier inventory in Austria, *The Cryosphere*, 9, 753-766, 2015.
- 671 Frei, C.: Interpolation of temperature in a mountainous region using nonlinear profiles and non-
672 Euclidean distances, *International Journal of Climatology*, 34, 1585-1605, 2014.
- 673 Frei, C., Christensen, J.H., Déqué, M., Jacob, D., Jones, R.G., and Vidale, P.L.: Daily precipitation
674 statistics in regional climate models: Evaluation and intercomparison for the European Alps,
675 *Journal of Geophysical Research*, 108(D3), 4124, doi: 10.1029/2002JD002287, 2003.
- 676 Gardent, M., Rabatel, A., Dedieu, J.-P., and Deline, P.: Multitemporal glacier inventory of the
677 French Alps from the late 1960s to the late 2000s, *Global and Planetary Change*, 120, 24-37,
678 2014.
- 679 Gardner, A. S., Moholdt, G., Cogley, J. G., Wouters, B., Arendt, A. A., Wahr, J., Berthier, E.,
680 Hock, R., Pfeffer, W. T., Kaser, G., Ligtenberg, S. R. M., Bolch, T., Sharp, M. J., Hagen, J. O.,
681 van den Broeke, M. R., and Paul, F.: A consensus estimate of glacier contributions to sea level
682 rise: 2003 to 2009, *Science*, 340 (6134), 852-857, 2013.
- 683 Kääb, A., Winsvold, S.H., Altena, B., Nuth, C., Nagler, T., and Wuile, J.: Glacier remote sensing
684 using Sentinel-2. Part I: Radiometric and geometric performance, and application to ice veloci-
685 ty, *Remote Sensing*, 8, 598, doi:10.3390/rs8070598, 2016.
- 686 Kienholz, C., Hock, R., and Arendt, A.A.: A new semi-automatic approach for dividing glacier
687 complexes into individual glaciers, *Journal of Glaciology*, 59 (217), 925-936, 2013.
- 688 Lambrecht, A., and Kuhn, M. (2007): Glacier changes in the Austrian Alps during the last three
689 decades, derived from the new Austrian glacier inventory, *Annals of Glaciology* 46, 177-184,
690 2007.
- 691 Marzeion, B., Champollion, N. ,Haeberli, W., Langley, K., Leclercq, P., and Paul, F.: Observation
692 of glacier mass changes on the global scale and its contribution to sea level change, *Surveys in
693 Geophysics*, 38 (1), 105-130, 2017.
- 694 Mölg, N., Bolch, T., Rastner, P., Strozzi, T., and Paul, F.: A consistent glacier inventory for the



- 695 Karakoram and Pamir region derived from Landsat data: Distribution of debris cover and
696 mapping challenges, *Earth Systems Science Data*, 10, 1807-1827, 2018.
697 Mölg, N., Bolch, T., Walter, A., and Vieli, A.: Unravelling the evolution of Zmuttgletscher and its
698 debris cover since the end of the Little Ice Age, *The Cryosphere*, 13, 1889-1909, 2019.
699 Oerlemans, J.: Extracting a climate signal from 169 glacier records, *Science*, 308, 675- 677, 2005.
700 Ohmura, A., Kasser, P., and Funk, M.: Climate at the equilibrium line of glaciers, *Journal of Glaci-
701 ology*, 38(130), 397-411, 1992.
702 Paul, F., Kääb, A., Maisch, M., Kellenberger, T.W., and Haeberli, W.: The new remote-sensing-
703 derived Swiss glacier inventory: I. Methods, *Annals of Glaciology*, 34, 355-361, 2002.
704 Paul, F., Kääb, A., Maisch, M., Kellenberger, T.W., and Haeberli, W.: Rapid disintegration of Al-
705 pine glaciers observed with satellite data, *Geophysical Research Letters*, 31, L21402, doi:
706 10.1029/2004GL020816, 2004.
707 Paul, F., Barry, R., Cogley, J.G., Frey, H., Haeberli, W., Ohmura, A., Ommanney, C.S.L., Raup,
708 B., Rivera, A., and Zemp, M.: Recommendations for the compilation of glacier inventory data
709 from digital sources, *Annals of Glaciology*, 50 (53), 119-126, 2009.
710 Paul, F., Frey, H., and Le Bris, R.: A new glacier inventory for the European Alps from Landsat
711 TM scenes of 2003: Challenges and results, *Annals of Glaciology*, 52 (59), 144-152, 2011.
712 Paul, F., Barrand, N. E., Baumann, S., Berthier, E., Bolch, T., Casey, K., Frey, H., Joshi, S. P.,
713 Konovalov, V., Le Bris, R., Mölg, N., Nosenko, G., Nuth, C., Pope, A., Racoviteanu, A.,
714 Rastner, P., Raup, B., Scharrer, K., Steffen, S., and Winsvold, S.H.: On the accuracy of glacier
715 outlines derived from remote sensing data, *Annals of Glaciology*, 54 (63), 171-182, 2013.
716 Paul, F., Winsvold, S.H., Kääb, A., Nagler, T., and Schwaizer, G.: Glacier remote sensing using
717 Sentinel-2. Part II: Mapping glacier extents and surface facies, and comparison to Landsat 8.
718 Remote Sensing, 8(7), 575; doi:10.3390/rs8070575, 2016.
719 Paul, F., Bolch, T., Briggs, K., Kääb, A., McMillan, M., McNabb, R., Nagler, T., Nuth, C.,
720 Rastner, P., Strozzi, T., and Wuite, J.: Error sources and guidelines for quality assessment of
721 glacier area, elevation change, and velocity products derived from satellite data in the Glaci-
722 ers_cci project, *Remote Sensing of Environment*, 203, 256-275, 2017.
723 Paul, F., Rastner, P., Azzoni, R.S., Diolaiuti, G., Fugazza, D., Le Bris, R., Nemec, J., Rabatel, A.,
724 Ramusovic, M., Schwaizer, G., and Smiraglia, C.: Glacier inventory for the Alps, online:
725 <https://doi.pangaea.de/10.1594/PANGAEA.909133>, 2019.
726 Pfeffer, W. T., Arendt, A.A., Bliss, A., Bolch, T., Cogley, J. G., Gardner, A. S., Hagen, J.-O.,
727 Hock, R., Kaser, G., Kienholz, C., Miles, E.S., Moholdt, G., Mölg, N., Paul, F., Radic, V.,
728 Rastner, P., Raup, B.H., Rich, J., Sharp, M.J., and the Randolph Consortium: The Randolph
729 Glacier Inventory: A globally complete inventory of glaciers, *Journal of Glaciology*, 60 (221),
730 537-552, 2014.
731 Rabatel, A., and 27 others: Current state of glaciers in the tropical Andes: a multi-century perspec-
732 tive on glacier evolution and climate change, *The Cryosphere*, 7, 81-102, 2013.
733 Rabatel, A., Ceballos, J.L., Micheletti, N., Jordan, E., Braithmeier, M., Gonzales, J., Moelg, N.,
734 Ménégoz, M., Huggel, C., and Zemp, M.: Toward an imminent extinction of Colombian glaci-
735 ers?, *Geografiska Annaler: Series A, Physical Geography*, 100 (1), 75-95, 2018.
736 Racoviteanu, A.E, Paul, F., Raup, B., Khalsa, S.J.S., and Armstrong, R.: Challenges in glacier
737 mapping from space: Recommendations from the Global Land Ice Measurements from Space
738 (GLIMS) initiative, *Annals of Glaciology*, 50 (53), 53-69, 2009.
739 Rastner, P., Bolch, T., Mölg, N., Machguth, H., Le Bris, R., and Paul, F.: The first complete inven-
740 tory of the local glaciers and ice caps on Greenland, *The Cryosphere*, 6, 1483-1495, 2012.
741 Raup, B., and Khalsa, S.J.S.: GLIMS Analysis Tutorial, 15 pp. Online at:
742 <http://www.glims.org/MapsAndDocs/guides.html>, 2007.



- 743 Reid, P. C., Hari, R.E., Beaugrand, G., Livingstone, D.M., Marty, C., Straile, D., Barichivich, J.,
744 Goberville, E., Adrian, R., Aono, Y., Brown, R., Foster, J., Groisman, P., Hélaouët, P., Hsu,
745 Kirby, R., Knight, J., Kraberg, A., Li, J., Lo, T., Myneni, R.B., North, R.P., Pounds, J.A.,
746 Sparks, T., Stübi, R., Tian, Y., Wiltshire, K.H., Xiao, D., and Zhu, Z.: Global impacts of the
747 1980s regime shift, *Global Change Biology*, 22(2), 682-703, 2016.
748 RGI consortium: Randolph Glacier Inventory – A Dataset of Global Glacier Outlines: Version 6.0,
749 GLIMS Technical Report, 71 pp., online at: glims.org/RGI/00_rgi60_TechnicalNote.pdf,
750 2017.
751 Sakai, A., Nuimura, T., Fujita, K., Takenaka, S., Nagai, H., and Lamsal, D. (2015): Climate re-
752 gime of Asian glaciers revealed by GAMDAM glacier inventory, *The Cryosphere*, 9, 865-880.
753 Smiraglia, C., Diolaiuti, G.A.: The new Italian glacier inventory, 1st ed., Ev-K2-CNR Publica-
754 tions, Bergamo, 2015.
755 Smiraglia, P., Azzoni, R.S., D'Agata, C., Maragno, D., Fugazza, D., and Diolaiuti, G.A.: The evo-
756 lution of the Italian glaciers from the previous data base to the new Italian inventory. Prelimi-
757 nary considerations and results, *Geografia Fisica e Dinamica Quaternaria* 38, 79-87, 2015.
758 Stumpf, A., Michéa, D., and Malet, J.-P.: Improved co-registration of Sentinel-2 and Landsat-8
759 imagery for earth surface motion measurements, *Remote Sensing*, 10(2), 160, doi:
760 10.3390/rs10020160, 2018.
761 Takaku, J., Tadono, T., and Tsutsui, K.: Generation of high resolution global DSM from ALOS
762 PRISM, *ISPRS International Archives of the Photogrammetry, Remote Sensing and Spatial In-*
763 *formation Sciences*, Vol. XL-4, 243-248, 2014.
764 Vaughan, D. G., Comiso, J. C., Allison, I., Carrasco, J., Kaser, G., Kwok, R., Mote, P., Murray, T.,
765 Paul, F., Ren, J., Rig- not, E., Solomina, O., Steffen, K., and Zhang, T.: Observations: Cry-
766 osphere, in: *Climate Change 2013: Physical Science Basis. Contribution of Working Group I*
767 to the Fifth Assessment Report of the Intergovernmental Panel on Climate Change, edited by:
768 Stocker, T. F., Qin, D., Plattner, G.-K., Tignor, M., Allen, S. K., Boschung, J., Nauels, A., Xia,
769 Y., Bex, V., and Midgley, P. M., Cambridge University Press, Cambridge, United Kingdom
770 and New York, NY, USA, 317-382, 2013.
771 Wouters, B., Gardner, A.S., and Moholdt, G.: Global glacier mass loss during the GRACE satellite
772 mission (2002-2016), *Frontiers in Earth Science*, 7 (96), doi: 10.3389/feart.2019.00096, 2019.
773 Zemp, M., Paul, F., Hoelzle, M., and Haeberli, W.: Alpine glacier fluctuations 1850-2000: An
774 overview and spatio-temporal analysis of available data and its representativity. In: Orlove, B.,
775 Wiegandt, E. and Luckman, B. (eds.): *Darkening Peaks: Glacier Retreat, Science, and Society*,
776 University of California Press, Berkeley and Los Angeles, 152-167, 2008.
777 Zemp, M., Frey, H., Gärtner-Roer, I., Nussbaumer, S.U., Hoelzle, M., Paul, F., Haeberli, W., Den-
778 zinger, F., Ahlstroem, A.P., Anderson, B., Bajracharya, S., Baroni, C., Braun, L.N., Caceres,
779 B.E., Casassa, G., Cobos, G., Davila, L.R., Delgado Granados, H., Demuth, M.N., Espizua, L.,
780 Fischer, A., Fujita, K., Gadek, B., Ghazanfar, A., Hagen, J.O., Holmlund, P., Karimi, N., Li,
781 Z., Pelto, M., Pitte, P., Popovnin, V.V., Portocarrero, C.A., Prinz, R., Sangewar, C.V., Sev-
782 erskiy, I., Sigurdsson, O., Soruco, A., Usubaliev, R., and Vincent, C.: Historically unprece-
783 dented global glacier changes in the early 21st century, *Journal of Glaciology*, 61 (228), 745-
784 762, 2015.
785 Zemp, M., Huss, M., Thibert, E., Eckert, N., McNabb, R., Huber, J., Barandun, M., Machguth, H.,
786 Nussbaumer, S.U., Gärtner-Roer, I., Thomson, L., Paul, F., Maussion, F., Kutuzov, S., and
787 Cogley, J.G.: Global glacier mass changes and their contributions to sea-level rise from 1961
788 to 2016, *Nature*, 568, 382-386, 2019.
789



790 Tables

791

792 *Table 1: Details about the Sentinel-2 tiles used to create the inventory, C.: Country.*

Nr.	Tile	Date	C.	Nr.	Tile	Date	C.	Nr.	Tile	Date	C.
1	32TMT	29 8 15	CH	9	32TMS	23 8 16	IT	17	31TGK	29 8 15	FR
2	32TNT	29 8 15	CH	10	32TNS	26 8 15	CH, AT	18	32TLR	29 8 15	FR, IT
3	32TNT	26 8 15	AT	11	32TNS	29 9 16	IT	19	32TLR	7 10 17	IT
4	32TPT	26 8 15	AT	12	32TPS	29 9 16	IT	20	32TMR	7 10 17	IT
5	32TQT	27 8 16	AT, IT	13	32TPT	26 9 16	IT	21	31TGK	29 8 15	FR
6	33TUN	27 8 16	AT, IT	14	32TQS	7 8 16	IT	22	32TLQ	23 8 16	IT
7	32TLS	29 8 15	CH, FR	15	32TQS	27 8 16	IT	23	32TLP	29 8 15	IT
8	32TMS	2 8 15	CH	16	33TUM	2 8 17	IT				

793

794

795 *Table 2: Glacier area and count per size class for the entire sample.*

Size class [km ²]	0.01-	0.02-	0.05-	0.1	0.1-	0.2-	0.5-	0.5-1	1-2	2-5	5-10	10-20	>20	All
	0.02	0.05	0.1		0.2	0.5								
Count	966	1060	723	532	520	244	177	103	48	16	5	4394		
Count [%]	22.0	24.1	16.5	12.1	11.8	5.6	4.0	2.3	1.1	0.4	0.1	100		
Area [km ²]	13.83	34.44	51.42	75.48	163.87	168.28	249.06	319.13	322.96	211.85	195.56	1805.8		
Area [%]	0.8	1.9	2.8	4.2	9.1	9.3	13.8	17.7	17.9	11.7	10.8	100		

796

797

798 *Table 3: Results of the multiple digitising experiment, listing for each of the five participants the mean glacier area (in km²) in the columns P1 to P5 along with the standard deviation in per cent (STD%). The last two columns provide the averaged values across all participants for each glacier and the last row gives total areas and their standard deviation across all glaciers and for each participant. The two values marked in blue are mean values derived from the other four participants. Red values mark highest values for glaciers larger and smaller than 1 km². Glacier ID 4 is missing as it was digitised as one glacier (with ID 5) by most participants.*

Gl-ID	P1	STD%	P2	STD%	P3	STD%	P4	STD%	P5	STD%	Mean	STD%
1	9.37	1.89	8.96	0.18	8.40	0.79	8.77	0.99	8.64	3.86	8.83	4.14
2	6.50	2.10	6.08	1.31	6.07	1.43	5.95	0.81	6.25	1.31	6.17	3.48
3	0.79	3.75	0.72	3.51	0.65	1.62	0.73	0.74	0.71	8.77	0.72	7.02
5	4.10	3.03	3.22	2.33	3.50	3.92	3.45	5.66	3.45	7.46	3.54	9.33
6	2.88	1.82	2.83	1.52	2.90	3.32	2.75	2.69	2.91	1.86	2.85	2.27
7	1.20	1.04	1.06	6.10	1.16	2.71	1.14	1.91	1.20	2.90	1.15	4.81
8	5.35	0.24	5.13	1.58	5.25	0.77	5.24	0.31	5.26	1.24	5.25	1.51
9	2.75	0.43	2.75	1.64	2.59	3.80	2.72	2.17	2.64	1.53	2.69	2.64
10	0.38	6.38	0.30	2.76	0.25	4.37	0.30	3.39	0.25	4.80	0.30	17.24
11	0.28	12.40	0.27	0.64	0.26	2.06	0.26	1.71	0.30	8.69	0.27	6.77
12	0.24	1.41	0.25	4.34	0.20	3.30	0.21	5.54	0.23	6.79	0.23	8.85
13	0.08	41.67	0.12	17.80	0.03	8.00	0.08	17.68	0.11	17.65	0.08	44.21
14	0.21	4.29	0.17	15.52	0.11	16.16	0.20	5.03	0.21	13.42	0.18	24.01
15	0.12	4.96	0.12	7.10	0.11	1.09	0.11	14.22	0.14	3.45	0.12	11.01
Sum	34.25	1.48	31.97	0.97	31.48	1.13	31.90	0.91	32.31	2.72	32.38	3.35

806

807



808

809 **Figure captions**

810 Fig. 1: Overview of the study region with footprints (colour-coded for acquisition year) of the Sen-
811 tinel-2 tiles used (see Table 1 for numbers).

812

813 Fig. 2: Comparison of hillshade views from a) the AW3D30 DEM and b) the TanDEM-X DEM
814 for a region around the Mt. Blanc/Monte Bianco. Glacier outlines are shown in red, data voids in
815 the TanDEM-X DEM are depicted as constantly grey areas. The AW3D30 DEM has been ob-
816 tained from <https://www.eorc.jaxa.jp/ALOS/en/aw3d30/index.htm> and is provided by JAXA. The
817 TanDEM-X DEM has been acquired by the TerraSAR-X/TanDEM-X mission and is provided by
818 DLR (DEM_GLAC1823).

819

820 Fig. 3: Results of the automated (clean ice) glacier mapping and threshold selection. a) band ratio
821 MSI band 4 / MSI band 11 (red/SWIR). b) Glacier classification results using different thresholds.
822 The lower values add some additional pixels, in particular in shadow regions where the threshold
823 is most sensitive. c) Blue band threshold to remove wrongly classified rock in shadow. The highest
824 value has been used resulting in a good performance in the left part of the image (white arrow) and
825 a bad one to the right (green arrow), where correctly classified ice in shadow is removed. d) Final
826 outlines (light blue) on top of the Sentinel-2 image in natural colours. All Sentinel-2 images shown
827 in the background: © Copernicus data (2016).

828

829 Fig. 4: Examples of challenging classifications in different countries. a) Debris cover delineation
830 (red) around Grossvenediger (Hohe Tauern) in Austria with raw extents (light grey) and outlines
831 from the previous national inventory (yellow). b) Tré-La-Tête Glacier (Mont-Blanc) with automati-
832 cally derived glacier extents (green), manually corrected outlines from 2015 (red) and outlines
833 derived from aerial photographs taken in 2008 (yellow). The S2 image from August 2015 is in the
834 background. c) Subset of the Orobio Alps in Italy (S2 image from September 2016), with evidence
835 of topographic shadow and debris covered glaciers. The inset shows an aerial photograph with bet-
836 ter glacier visibility but seasonal snow. d) S2 image from 2015 showing differences in interpreta-
837 tion of debris cover for Gaviolas glacier in Switzerland for the inventories from 2003 (yellow),
838 2008 (green) and 2015 (red). The inset shows a close-up of its lowest debris-covered part obtained
839 from aerial photography for comparison (this image is a screenshot from Google Earth). All Senti-
840 nel-2 images shown in the background: © Copernicus data (2016).

841

842 Fig. 5: Relative frequency histograms for glacier count and area per a) size class and b) aspect sec-
843 tor for all glaciers.

844

845 Fig. 6: Glacier area vs. a) minimum and maximum elevation and b) elevation range for all glaciers.



846

847 Fig. 7: Spatial distribution of median elevation (colour coded) for glaciers larger 0.5 km^2 . The inset
848 shows a scatterplot depicting glacier aspect (counted from North at $0/360^\circ$) vs. median elevation.

849

850 Fig. 8: Normalised glacier hypsometry per country as derived from the AW3D30 DEM.

851

852 Fig. 9: Visualisation of the strong glacier area shrinkage between 2003 (yellow) and 2015 (red) for
853 a sub-region of the Zillertal Alps (Austria and Italy). Sentinel-2 image shown in the background: ©
854 Copernicus data (2016).

855

856 Fig. 10: Overlay of glacier outlines from 2003 (black) and 2016 (yellow) showing the different
857 interpretation of glacier extents for the region around Sonnblickkees (SBK) in Austria. Sentinel-2
858 image shown in the background: © Copernicus data (2016).

859

860 Fig. 11: Overlay of glacier outlines from the multiple digitising experiment by all participants.
861 Colours refer to the first (yellow), second (red), third (green) and fourth (white) round of digitisa-
862 tion. Sentinel-2 image shown in the background: © Copernicus data (2016).

863

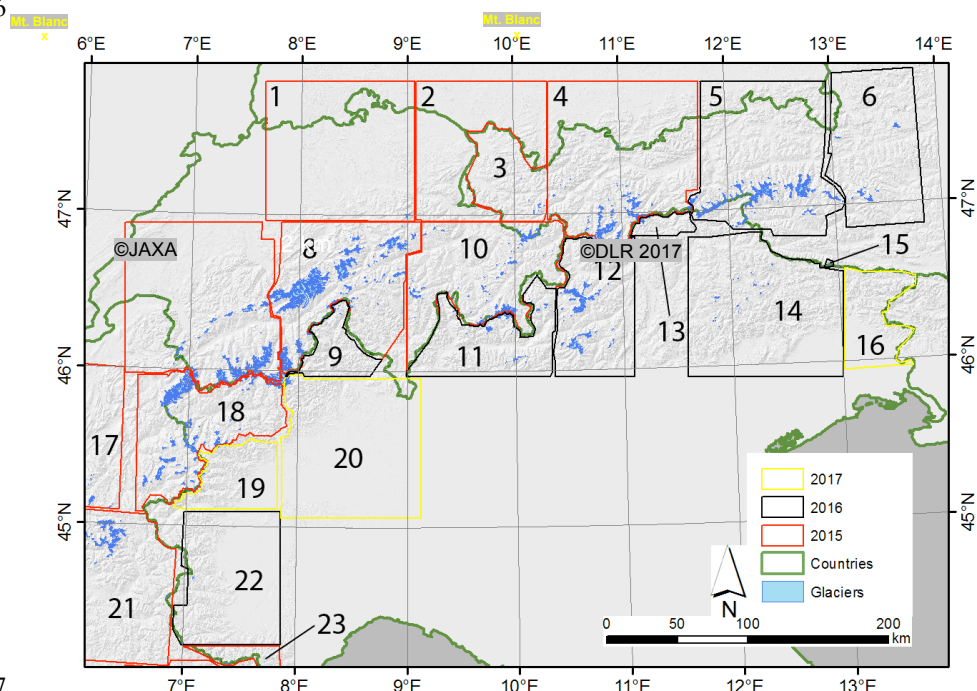


) b)

864

865 Figures

866

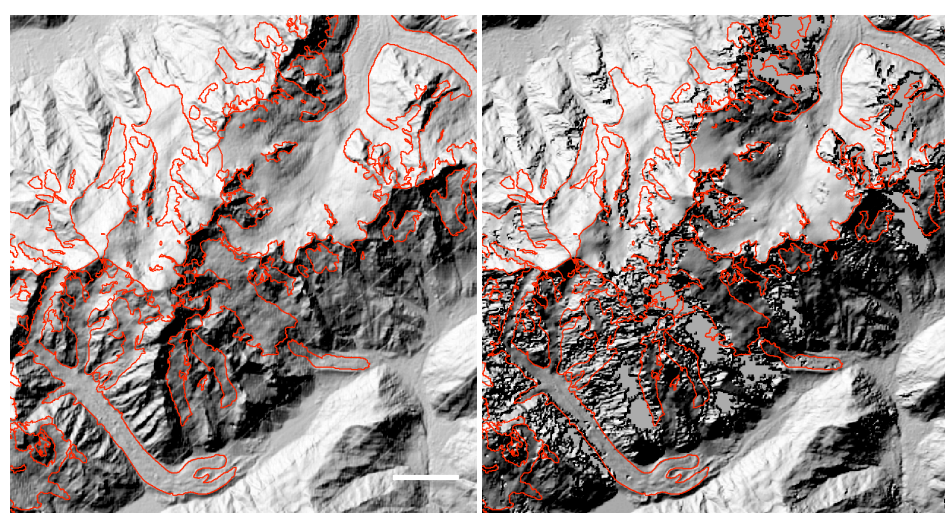


867

868 Figure 1

869

870



871

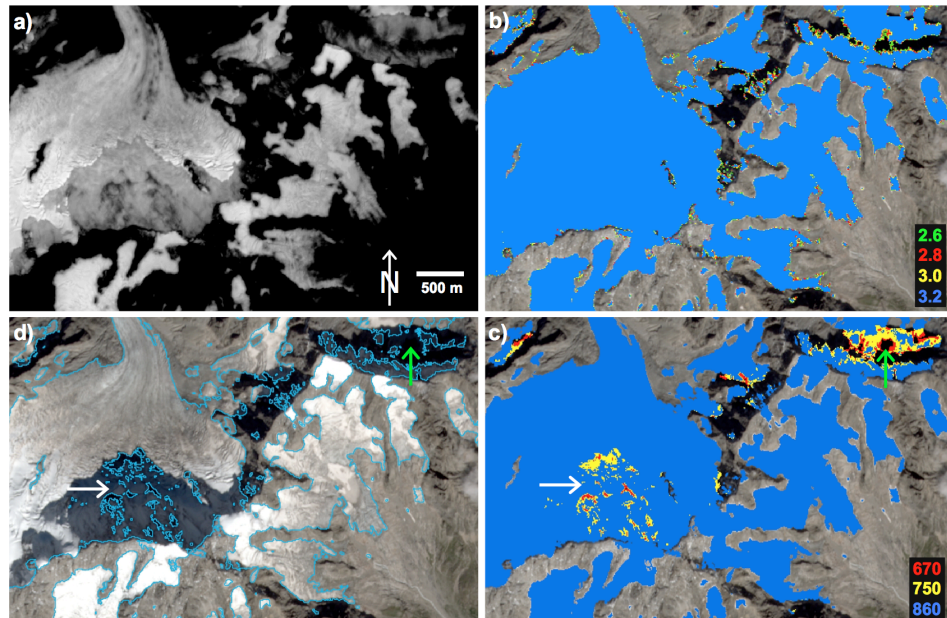
872 Figure 2

873

874



875



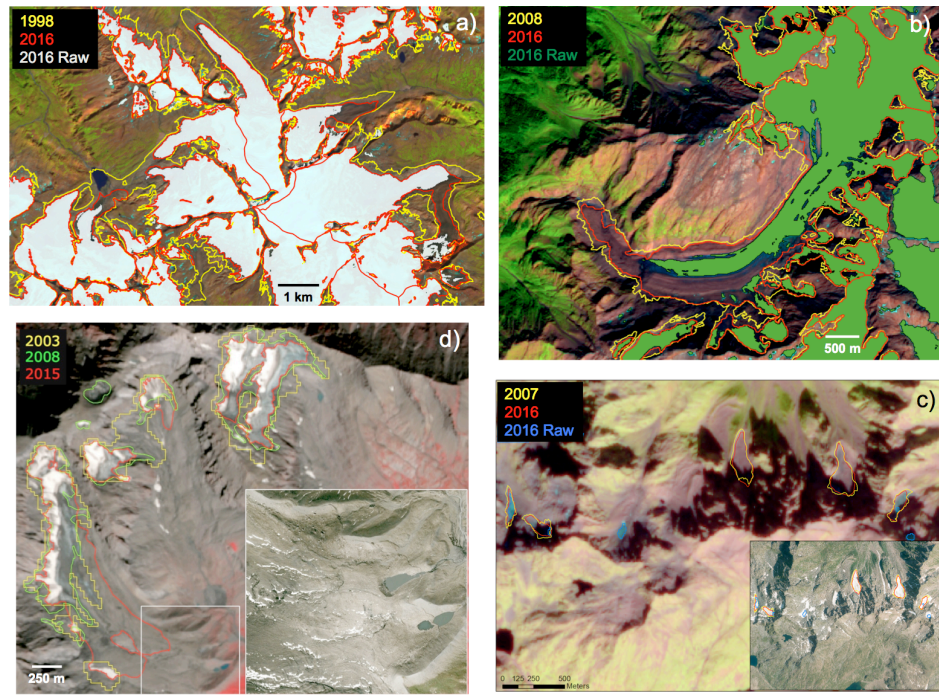
876

Figure 3

877

878

879



880

Figure 4

881



b)

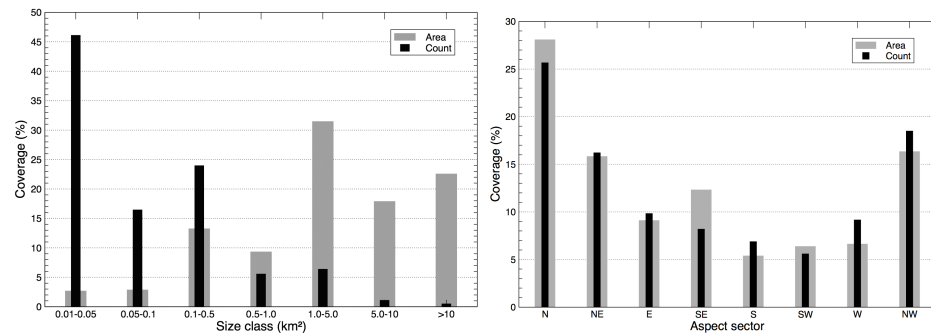
883

884

Figure 5

886

887

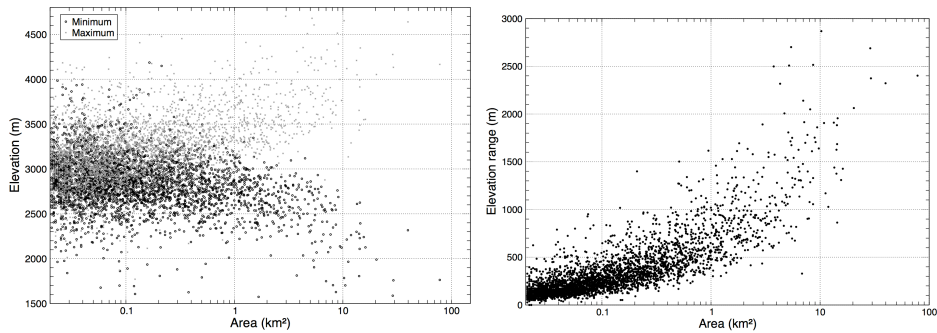


888

Figure 6:

890

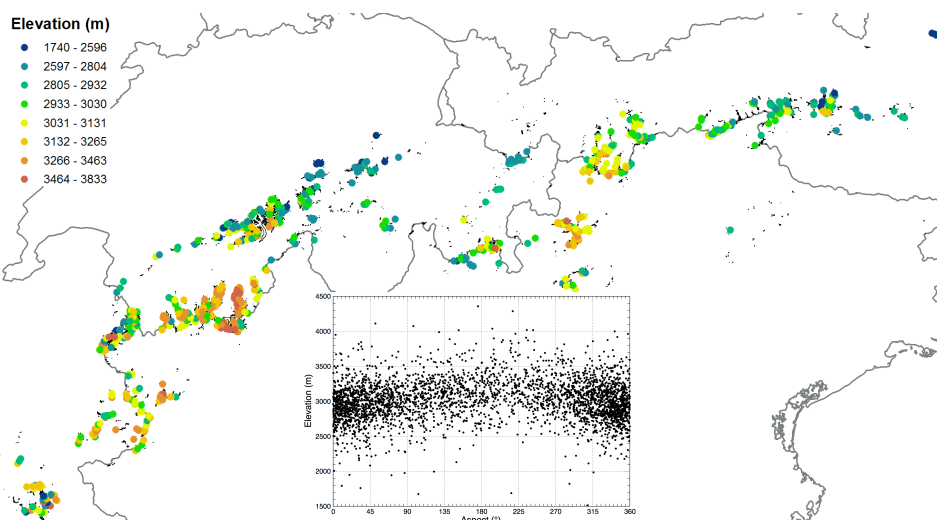
891



892

Figure 7

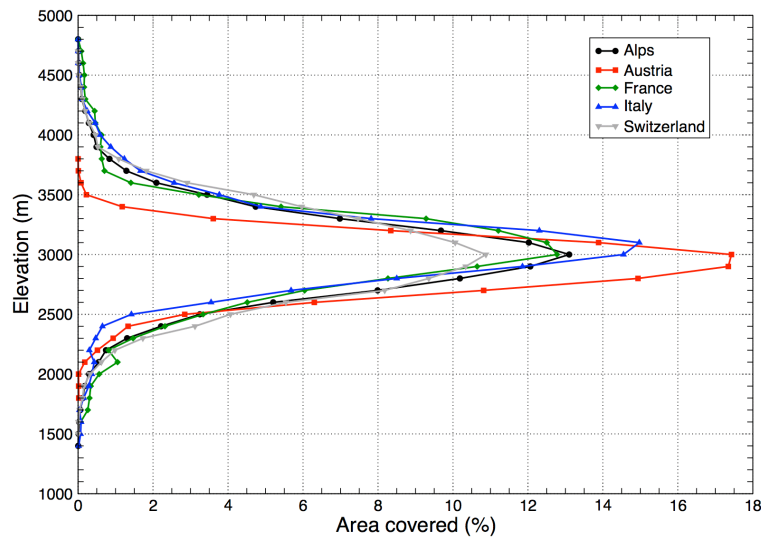
894





895

896



897

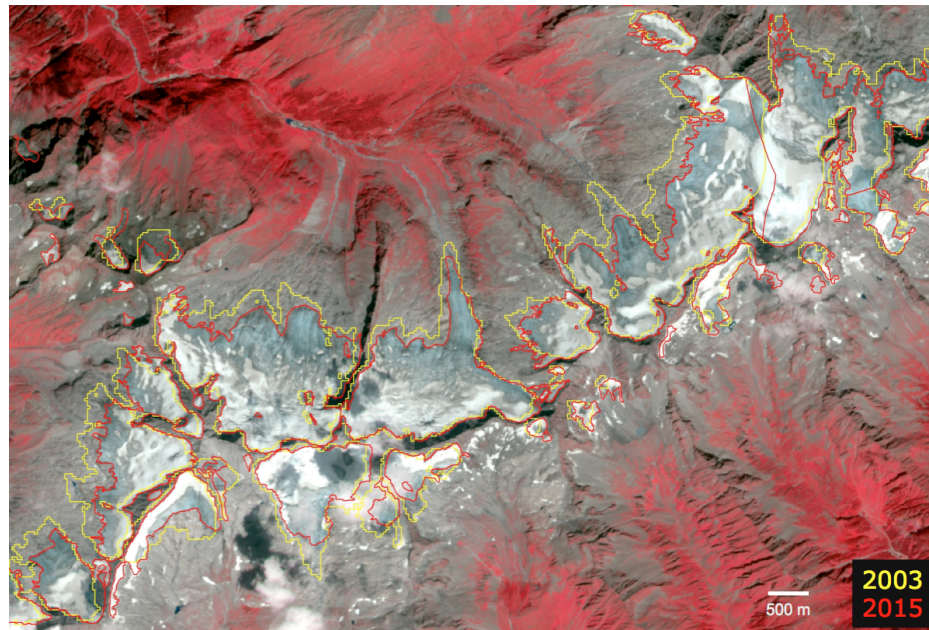
Figure 8

898

899

900

901

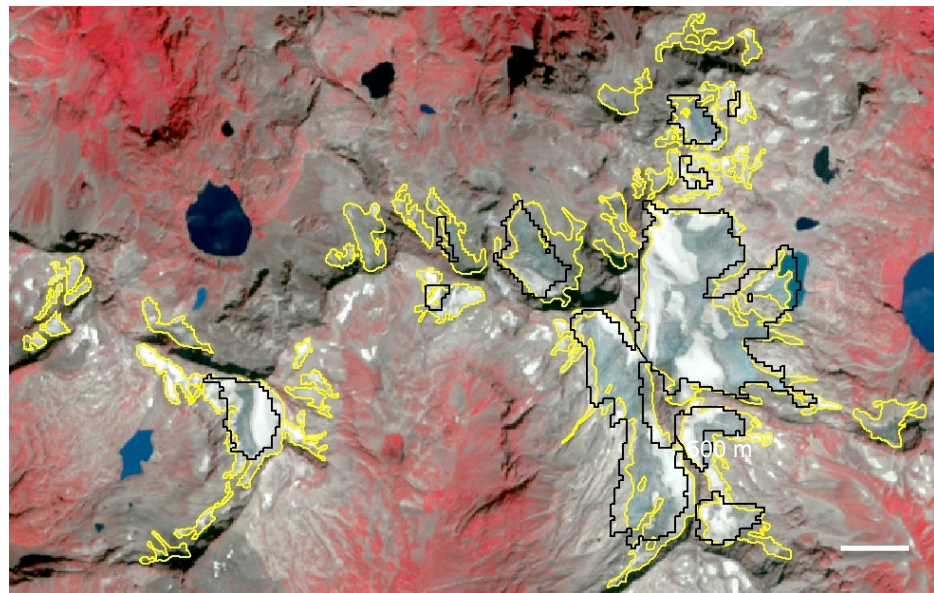


902

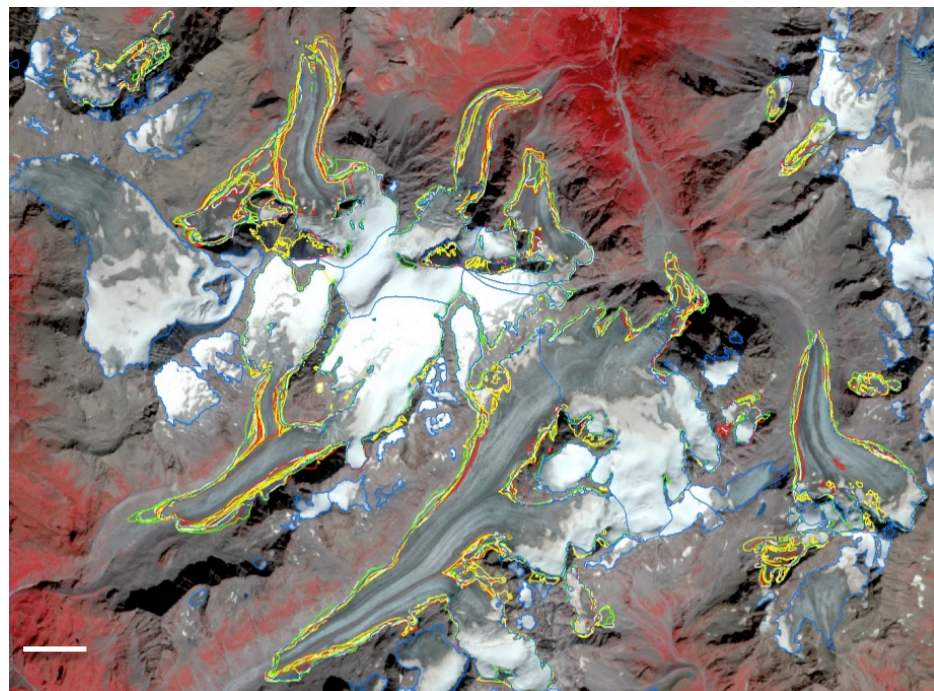
Figure 9

903

904



905
906 Figure 10
907
908



909
910 Figure 11
911